Journal of Hazardous Materials Advances 17 (2025) 100552

Contents lists available at ScienceDirect

Journal of Hazardous Materials Advances

journal homepage: www.elsevier.com/locate/hazadv

Asbestos fiber levels from remediation work

Anders Brostrøm [a,*], Henrik Harboe [b], Ana Sofia Fonseca [a], Marie Frederiksen [a], Pete Kines [a], William Bührmann [a], Jakob Hjort Bønløkke [c], Keld Alstrup Jensen [a]

[a] National Research Centre for the Working Environment, Copenhagen, Denmark
[b] Joblife, Kolding, Denmark
[c] Department of Occupational and Environmental Medicine, Aalborg University Hospital, Aalborg, Denmark

ARTICLE INFO

Keywords:
Asbestos fibers
Scanning electron microscopy
Asbestos remediation
Exposure
Filter sampling

ABSTRACT

Release of asbestos fibers during remediation and maintenance work remains a concern in many countries, as asbestos containing materials are often present in buildings predating their ban. Despite awareness of the adverse health effects from asbestos exposure, there is a lack of knowledge on concentrations resulting from typical asbestos remediation tasks, and on the minimum protection level needed. The aim of this study was to map asbestos exposure levels during removal of asbestos containing materials, in order to assess asbestos exposure levels and the adequacy of applied risk management measures, including choice of protective equipment. The investigated removal processes included asbestos containing facade panels, roof tiles, ceiling panels, tile adhesives, and insulation materials for pipes and boilers. All filter samples were analyzed by scanning electron microscopy coupled with energy dispersive X-ray spectroscopy. The highest asbestos concentration of 0.35 fibers/cm^3 was found during removal of tiles with asbestos adhesives, though levels exceeding the current Danish occupational exposure limit of 0.003 f/cm^3 were found in breathing zone samples at 11 of the 14 investigated sites. Even when considering 8 h time weighted average concentrations, levels were often found to exceed the occupational exposure limit, despite assuming a narrow exposure window, typically between 0.5 and 2 h due to high dust levels or short tasks. An additional objective was to provide guidance for decision-making in relation to two OEL options given in a recent EU Directive, where member states are also expected to transition from optical microscopy to electron microscopy for asbestos measurements.

Introduction

Asbestos is a common name for naturally occurring fibrous silicate minerals, found as the serpentine (chrysotile mineral) and amphibole (actinolite, amosite, anthophyllite, crocidolite, and tremolite minerals) groups (Hendry, 1965). When released from materials, amphibole fibers are seen mainly as straight, thin, and long single fibers, while chrysotile fibers are long thin and flexible fibrils that often occur in bundles (Strohmeier et al., 2010). Asbestos minerals have a high tensile strength, fire resistance, and excellent thermal and electrical insulator capabilities. Asbestos was therefore added to many products as a fire-proofing material, but also to increase strength and durability. Asbestos was especially used in the construction industry, during the mid to late 1900s. In 1991, the EU banned all use of amphibole asbestos minerals, while chrysotile was not banned until 2005, though several member states enforced amphibole and chrysotile bans even earlier, typically between 1980 and 1990 (Thives et al., 2022). However, asbestos containing materials (ACM) are still found in many buildings and houses throughout the EU, posing a significant risk during demolition and renovation tasks. In Denmark, the most common ACM include roof tiles, roofing felt, facade panels, ceiling panels, tile adhesives, and insolation materials used in ventilation, technical installations, and piping (Rasmussen, 2010). These materials are considered to pose no or minimal health risk as long as they are not disturbed, but during renovation and demolition tasks, considerable amounts of asbestos fibers are released into the air (Fonseca et al., 2022).

Asbestos fibers are considered hazardous if they have a length (L) > 5 μm, width (W) < 3 μm, and an aspect ratio L/W > 3, as such fibers can penetrate and deposit deep within the human respiratory tract (Suzuki et al., 2005). Asbestos fibers are insoluble, and those fulfilling the above mentioned WHO fiber criteria cannot be efficiently cleared from the lungs (Barlow et al., 2017). As a result, asbestos exposure is linked to

* Corresponding author.
E-mail address: abl@nfa.dk (A. Brostrøm).

https://doi.org/10.1016/j.hazadv.2024.100552
Received 9 September 2024; Received in revised form 6 November 2024; Accepted 25 November 2024
Available online 26 November 2024

adverse health effects such as pleural cancer, lung cancer, asbestosis, and pleural plaque (Paris et al., 2009; Pawełczyk and Božek, 2015; Ramada Rodilla et al., 2022). There is no known lower threshold of exposure for these illnesses, but the risk increases with rising exposure levels (Harris et al., 2021; Iversen et al., 2024). This means that even for daily work at the current Danish occupational exposure limit (OEL), which was recently lowered from 0.1 to 0.003 f/cm^3, there is an increased risk of cancer over time (Iversen et al., 2024). In Denmark there is a zero-tolerance of asbestos exposure, thus requiring airlocks, ventilation, disposable full body suits and gloves that are taped at the joints, as well as respiratory FP3 filtration for all asbestos remediation tasks. However, air sampling is not common practice in Denmark, meaning that exposure levels during remediation tasks are not readily available in the scientific or publically available literature. Consequently, though there is a regulatory requirement for protection, it is not apparent, what the applied protection factors of the mandated equipment should be to ensure an acceptable exposure level. This is further complicated by a lack of coherence between national guidance values across Europe on respiratory protection factors and by the numerous respiratory masks currently available on the market (HSE, 2013; INRS, 2011; Janssen et al., 2014; OSHA, 2009).

The aim of this study was to map the asbestos exposure levels in the breathing zone (BZ), near field (NF), and far field (FF) during different asbestos remediation tasks in Denmark, in order to improve our knowledge on external asbestos exposure concentrations in the workplace and applied precautionary measures. Results can be used to aid workers and employers in their future choice of protective equipment. In addition, an objective was to test the use of scanning electron microscopy (SEM) coupled with energy dispersive X-ray (EDS) spectroscopy for asbestos analysis, as a recent EU Directive require member states to transition from optical microscopy techniques to electron microscopy (The European Parliament and the Council of the European Union, 2023). In the Directive, member states are also given a choice of using either a limit value of 0.002 f/cm^3, which include asbestos fibers with widths between 0.2 and 3 μm or using a limit value of 0.01 f/cm^3 while including thin fibers with widths below 0.2 μm as well. An additional objective was therefore to identify challenges and issues for the two OEL-options, and thereby provide input for decision-making.

Materials and methods

Sites and sampling

The study was designed to include as many known ACM used in Denmark as possible and to include a variety of remediation tasks (Rasmussen, 2010). The frequency of different remediation tasks was not taken into account, nor was the type of building prioritized. Consequently, the study primarily included schools, apartment complexes, and terraced houses, while private detached houses were poorly represented (Table 1). A total of thirteen asbestos remediation sites and one asbestos waste disposal site were included from which 151 filter samples were collected and analyzed. Particles and fibers were collected onto gold-coated polycarbonate membrane filters with a pore size of 0.8 μm (I3 Membrane, Radeberg, Germany) at a flowrate of 1.9 L/min. An overview of the removed materials and tasks is given in Table 1, along with relevant site descriptors, while more detailed information from each sample can be found in the supporting information. The air exchange rates (AER) at each site (Table 1) were determined from known flowrates of the applied negative pressure units and estimated room size. However, some tasks were conducted outdoors, in which case high or low natural ventilation was marked, referring to windy and calm weather conditions. In a few cases, no information was available, which is marked as N/A.

The level of compliance to on-site health and safety control measures was documented through systematic observations at 10 of the sites using an app (nfa.dk/safetyobserver Andersen et al., 2018) with an adapted checklist in regards to compliance to: hazardous chemical information (e.g. warning signs, signage for use of personal protective equipment, labelling of hazardous materials), technical control measures (e.g. enclosing, shielding, wrapping, sealing, air cleaning/extraction, on-tool extraction), housekeeping (order and tidiness), proper use of personal protective equipment, and sanitary and first-aid facilities. One observation marking per object, area (max 50 m^2), machine, tool, person, etc. was scored as either 'correct' or 'not correct'. Upon completion of the walk- around in the areas where there were ongoing activities, the app generated a report and a safety index (0–100 % compliance), based on the percent of correct observations from the total number of observations. These observations showed high compliance levels across all 10 of the sites with an average compliance level of 91 %.

For BZ sampling, workers were equipped with a pump with the filter inlet located on the upper chest within 20 cm of the workers BZ. All stationary NF and FF filters were sampled at heights of approximately 1.5 m from the ground, using either tripod stands or strips to fasten the pump to scaffolding near the worker. Stationary NF measurements were

Table 1
Overview of ACM for removal, relevant site descriptors, estimated room size, estimated air exchange rate (AER), and the number of samples collected in the BZ, NF, and FF areas.

Site	ACM	Site description	Room size, m^3	AER, h^{-1}	BZ, #	NF, #	FF, #
1	Façade panels	Façade of public school	Outdoor	High, natural	4	4	2
2	Pipe insulation under roof	Insulation near roof at apartment complex	75, open to outside	Low, natural	5	3	3
3	Ceiling panels	Hallway at public school	120	N/A	6	2	2
4	Roof tiles	Roof of terraced house	Outdoor	High, natural	9	0	4
5	Ceiling panels	Hallway and classrooms at public school	629	14	1	1	3
6	Adhesive, kitchen tiles	Industrial kitchen at technical school	176	N/A	3	1	1
7	Ceiling panels	Hallway at apartment complex	331	N/A	6	2	1
8	Cleaning after roof removal	Roof of apartment complex	Outdoor	High, natural	3	1	2
9	Pipe insulation	Boiler room in basement at private house	40	25	3	3	5
10	Pipe and boiler insulation	Boiler room in basement of a public school	25	120	3	3	1
11	Adhesive, bathroom tiles	Bathrooms at a series of terraced houses	15	240	17	17	5
12	Asbestos waste disposal site	Special landfill for asbestos waste	Outdoor	High, natural	0	0	9
13	Ceiling panels	Hallway at a factory	250	7	4	2	4
14	Pipe insulation	Basement of an apartment complex	200	N/A	1	4	2

sampled from stands located 1–3 m from the worker, or as close as possible without interrupting the workflow. Stationary FF samples were collected outside the work zone to assess the risk of fiber dispersion in the immediate surroundings. The exact locations of the FF stations varied depending on the site, where most were positioned outside the airlock, near access roads, in neighboring rooms, or in adjacent walkways. Samples in the BZ were typically collected for approximately 2 h to prevent overloading. Sampling durations used at the NF were similar to those at BZ, while FF measurements as well as pre-activity measurements were longer, lasting approximately 4–5 h, with some extending to a full 8 h workday. The measurements were usually duplicated, so that the same sampling position was used in the morning and afternoon, in order to improve statistical validity.

SEM/EDS analysis

The collected samples were stored in their original filter cassettes until SEM analysis, where they were transferred to aluminum holders and inserted directly into the SEM for analysis. An Apreo 2C LoVac SEM (Thermofisher Scientific) was used at an acceleration voltage of 20 keV and a beam current of 0.4 nA. The images were acquired in Optiplan mode with the ETD detector, in order to minimize charging effects. Initial overview images were acquired at approximately 330 nm/pixel to assess particle load on the filters. Despite ISO guidelines (14966:2019) allowing only up to 10 % filter coverage, filters with a coverage of up to 50 % were included in this study, as they can still prove concentrations exceeding the OEL. A resolution of 50 nm/pixel was used for fiber identification to reliably detect objects down to 200 nm, while dimensions of recognized fibers were measured at higher resolution for greater precision. The largest available image dimension of 8192 × 5632 pixels was used to maximize the field of view for all images.

An Ultim Max 65 mm^2 EDS detector (Oxford Instruments) recorded spectra at a livetime of 5 s, while the Aztec software (Oxford Instruments) was used for quantification. Asbestos identification was based on a custom classification scheme using the determined elemental compositions, as standardized schemes are not available, due to variation between instruments. The developed scheme used normalized composition data so that Na + Si + Mg + Fe = 100 %. The criteria of the classification algorithm are given in Table 2 along with the ideal stoichiometric formulas for each of the asbestos minerals. Some asbestos minerals are a part of a mineralogical series, so their Mg and Fe content vary depending on their origin. For these minerals, two formulas are given, showing the range of compositions in terms of Mg and Fe content.

It should be noted that chrysotile asbestos not always conforms to the specified criteria due to its thin fibrils with limited EDS signal and since it is often associated with other particles that can contribute to the recorded spectra. Classification of chrysotile was therefore done both by composition and appearance.

The verified asbestos fibers were measured (length and width) and counted according to the rules described in the DS 2169 standard. The physical measurements were made either with the Aztec software (Oxford Instruments), ImageJ (Rueden et al., 2017), or with FibreDetect, which is a specialized program developed by the Bundesanstalt für Arbeitsschutz und Arbeitsmedizin (BAuA) (Peters, Torben et al., 2024). Airborne concentrations were determined as specified in ISO 14966:2019, including only asbestos fibers fulfilling the WHO criteria. A sufficient number of images or fibers were analyzed to ascertain airborne concentrations with 95 % certainty relative to the OEL. Ideally, work should be carried out significantly below the OEL, and measurements therefore have to be capable of quantifying concentrations at or below 10 % of the OEL (equivalent to detecting 10 fibers at 0.003 f/cm^3). Due to the extensive effort involved in analyzing the filter samples, this study focused on determining whether concentrations exceeded or were below the OEL, corresponding to three identified fibers at 0.003 f/cm^3.

Results and discussion

Particle coverage on filters

Of the 151 filters, 8 were discarded due to overload, and an additional 52 would have been discarded if ISO 14966:2019 had been strictly followed (particle coverage >10 % of the filter area). A total of 7685 images were taken at 50 nm/pixel along with approximately 1500 high resolution images and 10,365 EDS spectra. From these, 926 asbestos fibers were identified where 691 were within the WHO fiber definition.

A wide range of particle coverages were found on the collected filter samples (Fig. 1). Fig. 1A was acquired from a BZ filter sample collected during removal of asbestos-containing ceiling panels in a small hallway of a school. The sample had 65 % particle coverage after 1 h and 40 min of sampling, and as a result it was discarded. Fig. 1B originated from a BZ sample collected during removal of ceiling panels in a larger hallway at a different school. The particle coverage was 16 % after sampling for 1 h and 51 min. The fibers were still clearly distinguishable at this coverage, suggesting that the 10 % limit specified in ISO 14966:2019 is conservative. However, based on experience, a practical limit could be set at 20–25 % to allow longer sampling times and potentially shorten the analysis or at least reduce the risk of sample rejection. Fig. 1C shows

Table 2
Overview of the classification scheme for asbestos. The ideal stoichiometric formulas for each asbestos form are shown on the left, where some cover a range of possible compositions.

Elements	Si, at.%		Mg, at.%		Fe, at.%		Mg + Fe, at.%		Na, at.%	
Limits	Lower	Upper	Lower	Upper	Lower	Upper	Lower	Upper	Lower	Upper
Chrysotile $Mg_3Si_2O_5(OH)_4$	30	50	45	70	0	5	50	70	–	–
Amosite $(Mg_{2.1},Fe_{4.9})Si_8O_{22}(OH)_2$ $Fe_7Si_8O_{22}(OH)_2$	40	57	0	23	20	60	43	60	–	–
Anthophyllite $Mg_7Si_8O_{22}(OH)_2$ $Mg_5Fe_2Si_8O_{22}(OH)_2$	40	57	23	60	0	20	43	60	–	–
Actinolite $Ca_2Mg_{4.5}Fe_{0.5}Si_8O_{22}(OH)_2$ $Ca_2Mg_{2.5}Fe_{2.5}Si_8O_{22}(OH)_2$	57	70	5	38	5	38	30	43	–	–
Tremolite $Ca_2Mg_5Si_8O_{22}(OH)_2$ $Ca_2Mg_{4.5}Fe_{0.5}Si_8O_{22}(OH)_2$	57	70	25	43	0	5	30	43	–	–
Crocidolite $Na_2Mg_{1.5}Fe_{3.5}Si_8O_{22}(OH)_2$ $Na_2Fe_5Si_8O_{22}(OH)_2$	57	70	0	5	25	43	30	43	5	20

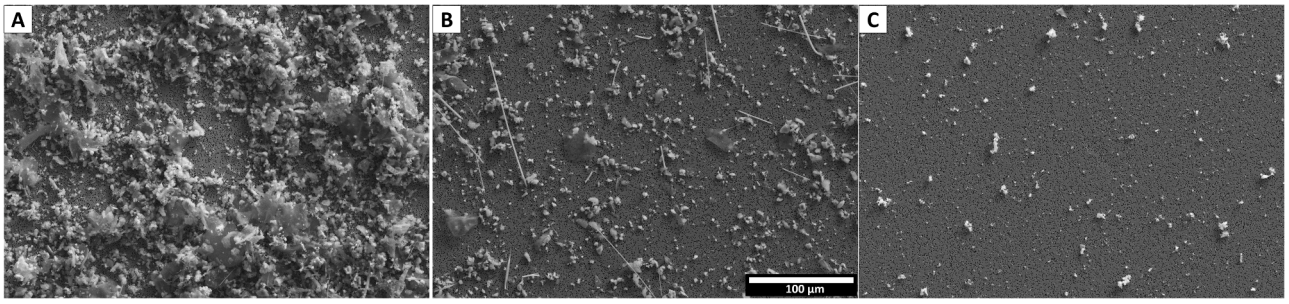

Fig. 1. Images acquired from BZ filter samples collected on site 3 (A), site 5 (B), and site 6 (C). All images were acquired using a resolution of 50 nm/pixel.

a BZ sample from an industrial kitchen where tiles with asbestos-containing adhesive were removed. The sample had a particle coverage of only 3 % despite a sampling time of 2 h and 26 min, which is longer than the samples in Fig. 1A and B. This demonstrates the challenge of determining optimal sampling times for asbestos analysis prior to sampling. To provide guidance for optimal sampling times, the filter coverage per hour of sampling on BZ filters for each of the included work processes were plotted (Fig. 2). The particle coverage was determined from overview images as the fraction of pixels related to particles relative to pixels corresponding to particle-free filter surface. The two pixel classes were differentiated based on a manually set global threshold. It should be mentioned that particle coverage is not a linear parameter, since initial particle deposition will always increase coverage, whereas particles depositing at a later stage can land on previously collected particles without adding to the overall filter coverage.

The dustiest processes in this study, namely sites 3, 6, and 11 (Fig. 2) require sampling times as low as 10–15 min, to ensure a coverage below 10 % as dictated in ISO 14966:2019. Most of the other work processes allow sampling times of 1–2 h without reaching a particle coverage of 10 %. However, such short sampling times lead to hundreds or thousands of images needing evaluation, which is poorly manageable via manual labor. This highlights a need for automated analysis assisted by artificial intelligence (AI) along with a revision of ISO 14966:2019 to potentially accept filters with a higher particle coverage, as a response to the recently lowered OEL.

Fiber types

Though many filters contained fibers (Fig. 1B) most of them were not asbestos but e.g., gypsum ($CaSO_4$), mineral wool, copper, zinc, or organic fibers (Fig. 3), which often occur at much higher concentrations than asbestos fibers. Especially gypsum and mineral wool fibers are very common in the construction industry, illustrated by the 10,365 recorded spectra resulting in only 926 verified asbestos fibers, which does not include fibers that were excluded based on visual inspection alone. Appearance can even vary significantly between the asbestos types, where the biggest differences are between the serpentine and amphibole asbestos forms (Fig. 3). Apart from visual inspection, asbestos fibers were distinguished based on the EDS classification scheme listed in Table 2, which is visually exemplified in Figure S1 in the supporting information along with normalized Si, Mg, and Fe concentrations for each of the 926 identified asbestos fibers.

Asbestos was detected at all sites except the asbestos waste disposal site (site 12) (Table 3). This could be a result of the outdoor measurements that were mainly sampled in the FF region. It was not possible to collect NF samples, as the pit used for dumping was constantly watered whenever new asbestos waste was unloaded. In addition, the pit was immediately covered with dirt after unloading, using a wheel loader, meaning that BZ samples would have originated from within the unloading trucks or inside the cabin of the wheel loader, and therefore not close to the source itself.

Chrysotile was the most prevalent type of asbestos, dominating at 6 out of the 13 sites where asbestos was found (Table 3). This is consistent with chrysotile being listed as the most commonly used form of asbestos in Denmark, making up approx. 89 % of asbestos usage, while amosite is listed at 10 % and crocidolite at 1 % (Raffn et al., 1989). Chrysotile was dominating in roof tiles as well as facade and ceiling panels. These products were typically produced at Dansk Eternit Fabrik A/S, a company producing mainly chrysotile containing products in Denmark from 1927 until 1988 (Miljøstyrelsen, 2023). However, chrysotile was not as dominant in our samples as expected. This could be a result of the study design, where focus was on covering as many different types of removal

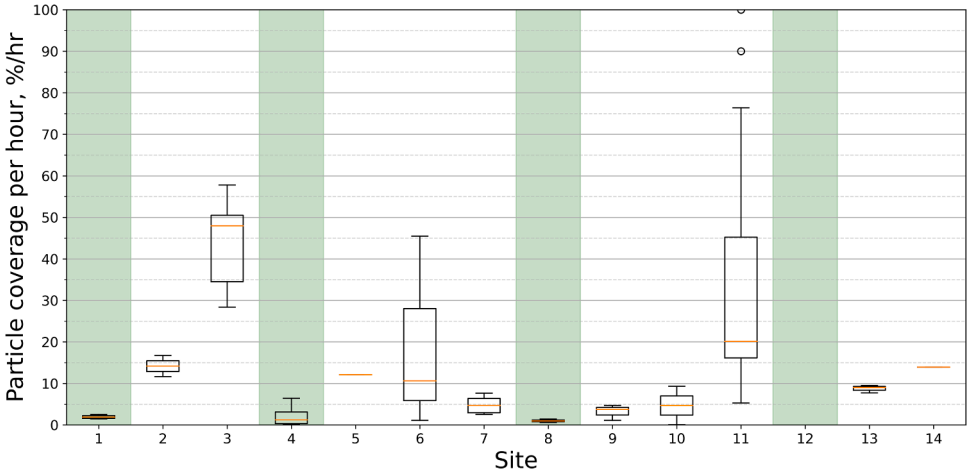

Fig. 2. Overview of particle coverage per hour estimated from BZ filter samples collected during asbestos removal activities at each of the 14 sites. Outdoor removal tasks are marked in green. No BZ filters were collected on site 12.

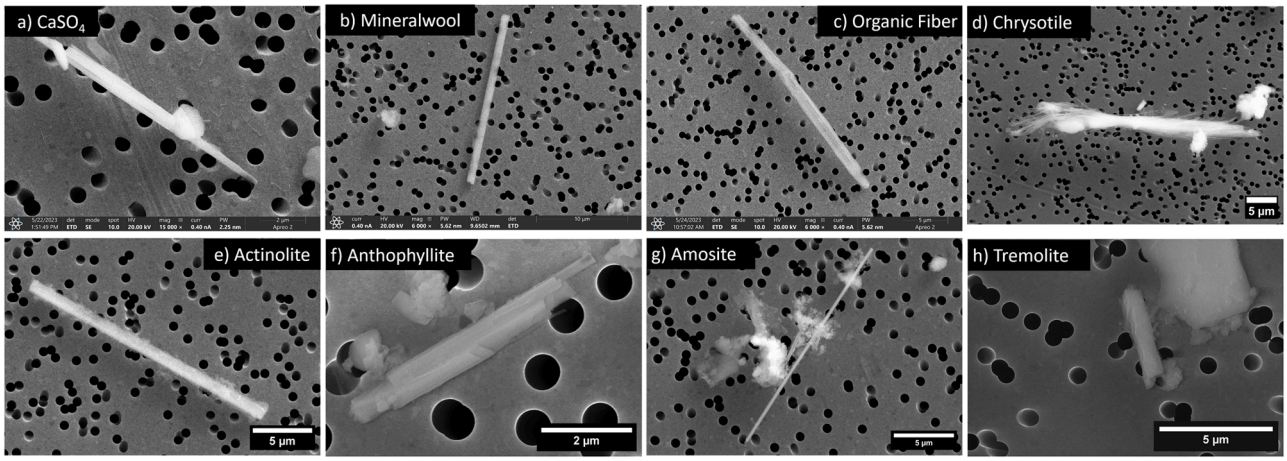

Fig. 3. High resolution images of recognized fibers from different filter samples.

Table 3
Overview of SEM/EDS results from each of the 14 sites, including percentage distribution of asbestos types.

Site	Number of filters	Number of filters with asbestos	Number of identified asbestos fibers	Chrysotile	Amosite	Anthophyllite	Actinolite	Tremolite
1	10	4	10	80 %	20 %	–	–	–
2	11	4	10	–	–	60 %	30 %	10 %
3	10	6	105	–	60 %	1 %	39 %	–
4	12	6	23	91 %	4.5 %	–	4.5 %	–
5	5	3	19	69 %	26 %	–	–	5 %
6	5	2	11	–	–	100 %	–	–
7	9	8	28	43 %	14 %	7 %	36 %	–
8	6	3	7	43 %	14 %	29 %	–	14 %
9	11	5	19	11 %	–	89 %	–	–
10	7	5	20	5 %	80 %	5 %	10 %	–
11	39	23	506	–	1 %	95 %	3 %	1 %
12	9	0	0	–	–	–	–	–
13	11	7	86	100 %	–	–	–	–
14	7	6	82	1 %	67 %	–	32 %	–

tasks as possible, rather than representing their frequency. Nonetheless, anthophyllite was found to dominate four sites, involving removal of asbestos-containing tile adhesive as well as in pipe and boiler insulation. This is somewhat surprising, as it is a rare form of asbestos that has only been commercialized to a limited extent outside Finland (Ilgren and Hoskins, 2017). In Finland however, it occurs naturally and has been used for centuries (Ilgren and Hoskins, 2017; Raffn et al., 1989). Amosite was the primary asbestos type at three locations, which is more consistent with it making up approx. 10 % of the reported asbestos use in Denmark (Raffn et al., 1989). Amosite was dominating during removal of pipe and boiler insulation, though it was also found when removing ceiling panels. Actinolite and tremolite were present on many sites, but were never the most frequent forms. Several types of asbestos were found at all sites, which was expected, as naturally occurring asbestos minerals often contain several different asbestos types (Van Gosen, 2007).

Fiber dimensions and adequacy of existing definitions

In addition to the elemental composition, length and width were measured for all 926 recognized asbestos fibers (Fig. 4). A significant uncertainty of the reported dimensions are expected for chrysotile fibers, which typically occur in bundles, are flexible, and often associated with other particles that can contribute to the EDS signal.

Most of the identified fibers fall within the WHO criteria, but a significant fraction is shorter than the required 5 µm, while a few have widths exceeding the 3 µm limit (Fig. 4). Only a single fiber was discarded due to a low aspect ratio, while fulfilling the length and width criteria. Though no clear trends in fiber dimensions were found when comparing sites (Fig. 4), some statistically relevant differences were found when grouping the sites based on type of ACM (Figs. S2–S4). The sites were clustered into five groups namely: facade panels, pipe insulation, roof tiles, ceiling panels, and tile adhesives. The longest fibers on average were observed for removal of facade panels (23.7 ± 16.1 µm) followed by removal of pipe insulation (18.8 ± 18.3 µm), roof tiles (17.8 ± 15.1 µm), and ceiling panels (12.8 ± 8.8 µm), while the shortest fibers were observed for removal of tiles with asbestos containing adhesives (8.0 ± 6.5 µm). Within the task groupings little to no statistically relevant variation was observed (Fig. S3), indicating that each specific task and ACM release asbestos fiber populations with similar dimensions. However, significant differences were found when comparing length datasets of the different task groupings (Fig. S4), where especially the task involving tile adhesives was found to be statistically distinct due to the much shorter fibers. Fiber widths showed less variation than fiber length with median widths ranging from 1.0 µm at site 1 to the lowest of 0.41 µm at site 3. Also, when comparing the different site and task groupings (Figs. S3 and S4), there were fewer combinations resulting in a statistical difference. This indicates that the fiber width is less affected by the removal method and/or ACM of origin.

When grouping the fiber length and width data based on asbestos type, the fiber width medians vary only from 0.4 to 0.6 µm, while the fiber length medians vary from 4.0 to 12.0 µm (Fig. S5). However, a statistically relevant difference was observed between several of the asbestos types (Fig. S6). Tremolite was found to be significantly shorter than all but the anthophyllite asbestos, while chrysotile was found to be significantly thicker than all but tremolite. The thick chrysotile fibers indicate that mainly larger bundles were observed during analysis, and could mean that single fibrils were either not released or have been

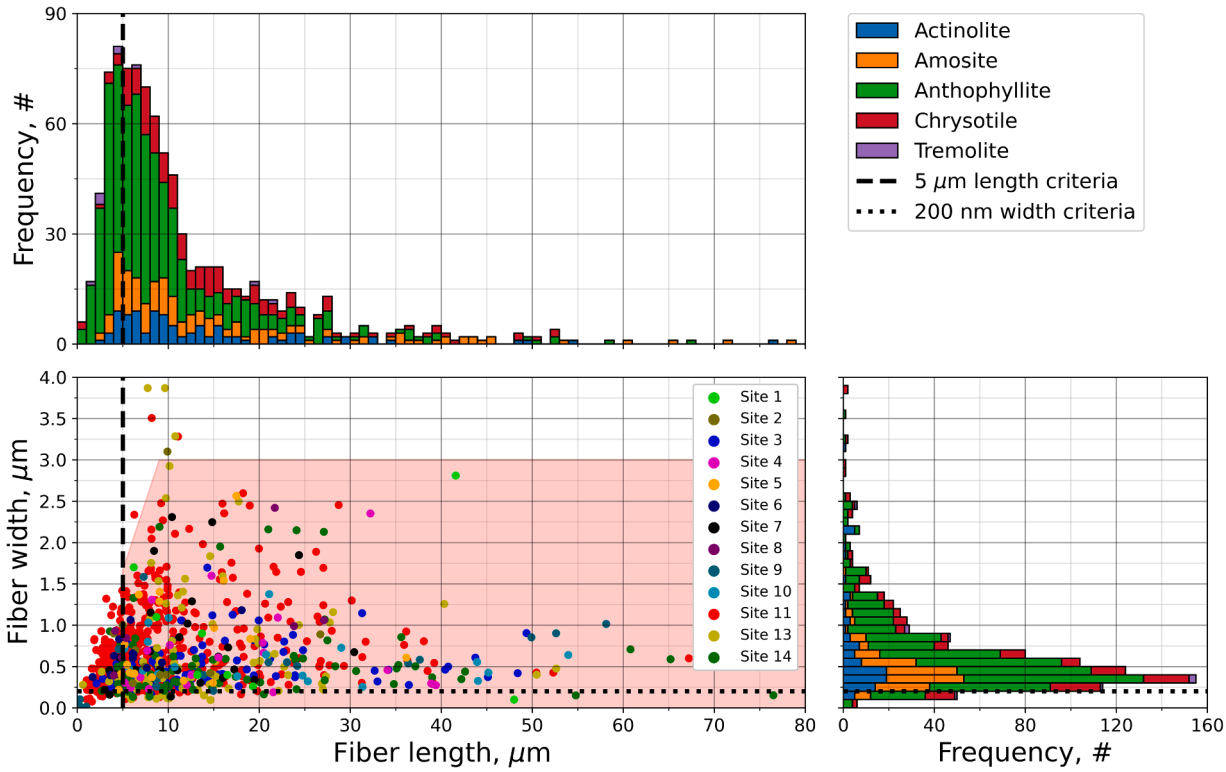

Fig. 4. Top: Histogram of asbestos fiber lengths in 1 μm bins colored according to asbestos type. The 5 μm WHO length criteria is marked as a dashed line. Bottom left: Scatter plot of asbestos fiber lengths and widths colored according to site. Red area marks dimensions fulfilling WHO fiber criteria. Bottom right: Histogram of asbestos fiber widths in 100 nm bins colored according to asbestos type. Estimated resolution limit of 200 nm is marked by dotted line.

overlooked at the applied pixel resolution of 50 nm/pixel in the sample screening procedure. The overall fiber width distribution peaked at a width of 300–400 nm (Fig. 4), so well before reaching the estimated resolution limit of 200 nm. At the same time, the fiber frequency drops quickly at widths below 300 nm. A similar width distribution was found for amphibole fibers by Ervik et al. (2023), when analyzing samples from several asbestos removal tasks in Norway. However, they found a dominance of thin asbestos fibers (TAF) (0.01 μm < W < 0.2 μm) when chrysotile was the main asbestos type. In a large study performed in France, a total of 71 sites were assessed by transmission electron microscopy, using an indirect method (Eypert-Blaison et al., 2018). Here, it was found that TAF exceeded the level of WHO fibers, but these were almost exclusively chrysotile fibers. Fibers thinner than 200 nm were at the limit of resolution with the settings used in this study, so thin chrysotile fibrils could have been unresolved and overlooked.

The overall length distribution founds in this study peaks at 5 μm (Fig. 4), which coincides with the WHO fiber length criteria. In the study by Ervik et al. (2023) fibers shorter than 5 μm were excluded, however, both for indoor and outdoor measurements they found the highest concentrations at a length of 5.0–5.9 μm, which agrees with our observations. In a French study by Eypert-Blaison et al. (2018) short asbestos fibers (SAF) (3 μm < L < 5 μm) were differentiated from TAF and WHO fibers. They found that SAF made up 68 % of all identified asbestos fibers, including both serpentine and amphibole fibers. In comparison, this study found that SAF constituted 25.4 % of the identified asbestos fibers. If the overall length distribution from this study (Fig. 4) is a general case, then even a small shift in the length distribution can have a significant influence on the reported asbestos concentration. From an analytical perspective, ideally the cut-off should lie at the upper or lower tail of the distribution, to either include or exclude the majority of the airborne asbestos fibers, ensuring less variation in the reported concentrations. It may therefore be necessary to update the WHO fiber length criteria, taking observed length distributions into account. However, this study alone is insufficient to confirm that the reported length distribution accurately represents asbestos fibers released from renovation tasks in general. Further studies and additional data are required to determine if the observed distribution is typical, and if so, to substantiate a new fiber definition that effectively assesses the risk of airborne asbestos fiber exposure.

Asbestos concentrations in air

A few samples were collected before initiating the remediation activities at sites 1, 2, 4, 9, 10, and 11. Ongoing construction work at some of the sites, resulted in deposition of particles and other fibers on the filters, but no asbestos fibers were detected in any of the samples. This suggests that asbestos fibers are not released until the ACM is disturbed or compromised during remediation work, as expected.

Airborne asbestos concentrations for each of the 14 sites, were divided into BZ, NF and FF samples (Fig. 5). Only filters collected during asbestos remediation work were included when calculating airborne concentrations. Concentrations corresponding to the limit of detection (LOD) were reported for cases where no asbestos fibers were positively identified. For such cases, the actual asbestos concentration is lower than the reported LOD with 95 % certainty. The LOD was typically at or below 0.001 f/cm^3, varying based on the analyzed filter area and collection time.

Asbestos was found at all sites except site 12, even when the work was performed outdoors. In general, high dust levels also showed high asbestos concentrations. The highest concentrations across all sites were found in the BZ samples, compared to NF and FF samples. At 11 of the 14 sites, concentrations exceeded the Danish OEL in one or more BZ samples, and some also exceeded the previous Danish OEL of 0.1 f/cm^3.

When considering the different tasks, sites 1, 4, and 8 involved outdoor asbestos work with removal of facade panels and roof tiles. In addition, site 2 involved removal of pipe insulation in a building, where

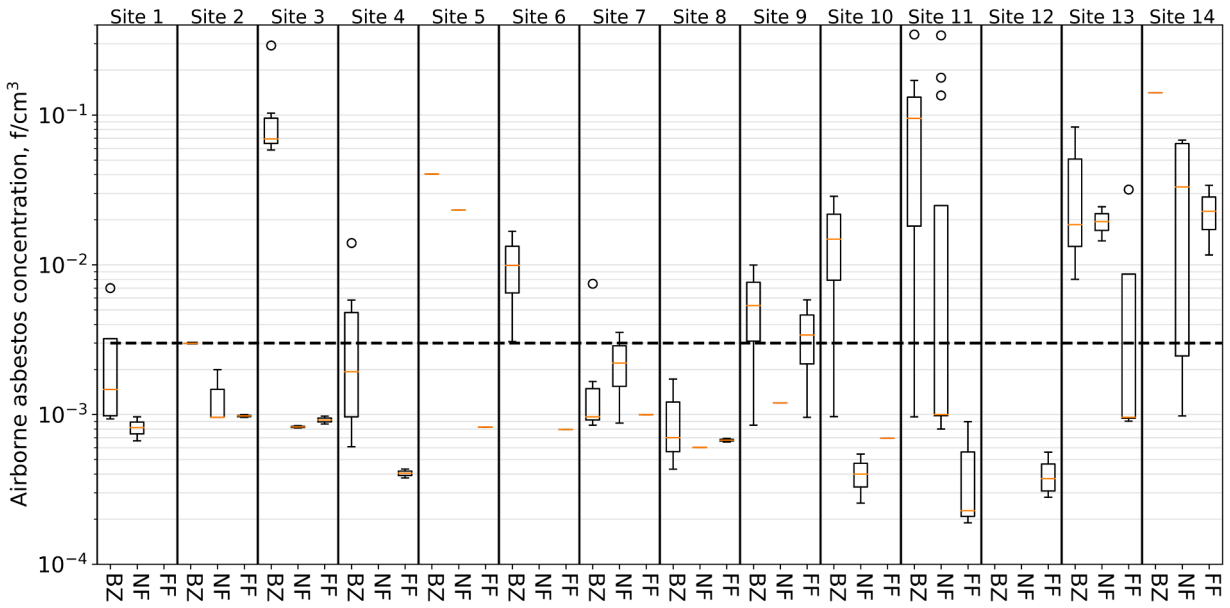

Fig. 5. Airborne asbestos concentrations in the BZ, NF, and FF locations at each of the 14 sites. The dashed line marks the current Danish OEL of 0.003 f/cm^3.

doors and windows had been removed, thus mimicking outdoor work conditions. These sites had the fewest samples with verified asbestos fibers and resulted in some of the lowest reported concentrations. This was similarly observed when the roof was covered with a tent for weather protection, as was the case at site 8. Filters from the NF and FF stations at these sites were all below the OEL, because of high air exchange and dilution rates typical for outdoor work. However, concentrations above the limit value were still measured in some BZ filters collected at sites 1, 2, and 4. The highest concentration of 0.014 f/cm^3 was measured at site 4, exceeding the Danish OEL by a factor of 4.7. The average concentration of all BZ samples with positive asbestos identification was 0.0044 f/cm^3, which is significantly lower than the average of 0.1 f/cm^3 reported by Ervik et al. (2023) both in the BZ and NF during outdoor removal of asbestos containing cement roof sheets, slate shingles, and wall shingles. An even higher average concentration of 0.2 f/cm^3 was reported in a French study during roof ACM removal (Eypert-Blaison et al., 2018). Ervik et al. also collected FF samples and found levels below LOD similar to our observations (Ervik et al., 2023). However, they also investigated a roof renovation with a plastic cover for weather protection similar to site 8 and reported a FF concentration of 0.05 f/cm^3 while concentration below LOD were found in this study. The higher concentrations found in France and Norway could be a result of weather conditions, where windy conditions are expected to lower concentrations. Alternatively, the higher concentrations could be a result of roof deterioration, as it has been shown that older ACM in poor condition e.g. cement roof sheets and slate shingles has more exposed asbestos fibers and are more brittle, which result in a higher release (Ervik et al., 2021).

Indoor removal of ceiling panels at sites 3, 5, 7 and 13, showed high asbestos concentrations in BZ filters, except for site 7 where concentrations were generally below the OEL. The BZ concentrations on sites 3, 5, and 13 ranged from 0.008 to 0.292 f/cm^3 with an average of 0.081 f/cm^3, which is 27 times higher than the current OEL. Similar concentrations were reported in France, with an average WHO asbestos fiber concentration of 0.188 f/cm^3 during ceiling panel removal, and double that when including TAF (Eypert-Blaison et al., 2018). At sites 5 and 13, the NF measurements were similar to the BZ measurements, while they were low for site 3 and 7. For sites 3, 5 and 7 the FF measurements were all below the OEL, while one out of four FF measurements at site 13 was significantly above OEL. These results indicate high exposure during ceiling panel removal in both BZ and NF.

The highest reported asbestos concentrations were at site 11, involving removal of bathroom tiles with asbestos adhesives. Here, BZ concentrations ranged from 0.005 to 0.345 f/cm^3 with an average of 0.108 f/cm^3, which is 36 times higher than the limit value, though the highest measured concentration was more than 100 times the OEL. The small size of the bathrooms (15 m^3), combined with the dusty work process contributed to excessive dust levels. Consequently, many filters from site 11 were overloaded, necessitating reduced collection times of 15–30 min for many samples. Due to the small bathroom size, all FF samples were collected outside the airlock, resulting in only one verified asbestos fiber. Site 6 involved a similar task in an industrial kitchen, where tiles with asbestos containing adhesive were removed, but dust levels were considerably lower than at site 11 due to a larger room size of approx. 175 m^3. The asbestos levels found in the two BZ filters from site 6 showed levels of 0.0031 and 0.0167 f/cm^3 corresponding to levels at and 5.6 times higher than the OEL, respectively. Site 6 had only one NF and one FF measurement, but the NF filter was overloaded, and no asbestos fibers were observed on the FF sample. Average concentrations of 0.066 f/cm^3 were found from 16 sites involving removal of wall tiles with asbestos adhesive in France, increasing to 0.26 f/cm^3 when including TAF, which aligns with the finding of this study.

Asbestos removal from boilers and pipe work in basements were conducted at sites 9, 10, and 14. At sites 9 and 10 the ``bag method'' was used, but it was not utilized at site 14. In the “bag method”, the section of piping with asbestos insulation is tightly wrapped in a plastic bag and sealed at both ends. The pipe is then cut next to the seals, where only mineral wool is expected, which is removed before cutting. The cut is made without compromising the plastic bag, so that all asbestos material should be sealed within the plastic bag, eliminating or minimizing release of fibers into the air.. At sites 9 and 10, asbestos levels in the BZ samples ranged from 0.005 to 0.029 f/cm^3 with an average of 0.015 f/cm^3, which is 5 times higher than the OEL. At site 14, where the “bag method” was not used and pipes were cut directly, only a single BZ sample was collected, which showed a concentration of 0.141 f/cm^3, which is 47 times the OEL. This suggests that while the “bag method” can significantly reduce asbestos levels, exposure cannot be eliminated entirely. This could be due to insufficient sealing of bags or residual asbestos present in the cut areas. When using the “bag method” at sites 9 and 10, the NF and FF measurements were primarily below the OEL. On the other hand, both the NF and FF measurements were very high at site 14, where the “bag method” was not used. However, both the NF and FF

stations were located within the working area at site 14, while FF stations at sites 9 and 10 were outside the enclosed area. Average concentrations of 0.1 f/cm^3 and 0.02 f/cm^3 were reported for similar tasks in Norway and France (Ervik et al., 2023; Eypert-Blaison et al., 2018), respectively, which are consistent with the findings of this study.

It is important to note that the current OEL in Denmark is based on an 8-h time weighted average (TWA). Most measurements in this study were considerably shorter than 8 h, either to avoid filter overloading or because the tasks themselves did not take 8 h. Regardless, exposures exceeding the OEL were still observed for TWA concentrations (Fig. S7), even when assuming workers were exposed to asbestos only during sampling, which in some cases were as short as 15–30 min. Within the remainder of the 8 h, it was assumed that workers were exposed to concentrations of 0 f/cm^3. These results are therefore not valid if workers were exposed to asbestos outside the sampling period. TWA concentrations exceeding the OEL were found at sites 3, 5, 11, 12, and 14. These sites involved ceiling panel removal (sites 3, 5, and 14), removal of tiles with asbestos adhesive (site 11), as well as removal of piping with asbestos insulation in a basement without using the "bag method" (site 14). This indicates that even relatively short tasks of less than 2 h can result in TWA exposure levels that exceed the current OEL.

Samples were also collected during and after cleaning processes at sites 5, 9, 10, and 11. At site 5, two samples were collected at the FF location after the activities had ended. One asbestos fiber was found, meaning that the airborne concentration with 95 % certainty lies between 0.0002 and 0.004 f/cm^3, and therefore most likely lower than the current OEL. No asbestos fibers were found on site 9 during cleaning activities the day after ACM removal, but here the asbestos levels were also relatively low during the remediation itself. At site 10, a single BZ sample was collected during the cleaning process but before the airlock was removed; it had a concentration of 0.075 fibers/cm^3, 25 times higher than the OEL, and higher than the levels during the ACM removal. At site 11, two BZ and two NF samples were collected during the first cleaning process. One of the BZ samples was overloaded, while the other was 33 times higher than the OEL with a concentration of 0.10 f/cm^3. One NF sample was below the OEL, while the other was 3 times higher at a concentration of 0.01 f/cm^3. In addition, six samples were collected during the second cleaning process at site 11, divided into 3 NF and 3 BZ samples. All BZ samples exceeded the OEL, with values ranging from 0.115 to 0.345 fibers/cm^3. For the NF samples, two showed concentrations of 0.025 and 0.135 fibers/cm^3 respectively, while no asbestos fibers were found on the last filter. Nevertheless, it is evident that asbestos exposure remains a significant risk during cleaning processes after ACM removal, with some concentrations exceeding those during removal itself. Therefore, thorough cleaning procedures and use of effective protective equipment are also crucial during cleaning and should be prioritized.

Choice of respiratory protective equipment

Though respiratory protective equipment (RPE) is mandated during asbestos remediation tasks in Denmark, no specific recommendations are provided on the choice of equipment. Instead, RPE manufacturers must demonstrate the assigned protection factor (APF) of their products. General guidelines are available in e.g. England, USA, and France, where the Health and Safety Executive (HSE) HSE (2013), OSHA (2009), and INRS (2011) respectively, have provided overviews of different types of RPE and their APFs. However, these reported APFs vary between institutions, as shown in Table 4, which lists APF guidance values from HSE and OSHA for selected RPE.

Both HSE and OSHA classify RPE into several groups including half masks, full facepieces, helmets/hoods, which cover the entire head, and loose-fitting facepieces, where excess air is emitted along the edge of the mask due to overpressure within the mask. In addition, both institutions differentiate between manual air-purifying respirators (APR), powered APR (PAPR), supplied-air respirators (SAR), where air is supplied from a hose leading to fresh air, and finally self-contained breathing apparatus (SCBA), where air is supplied from a pressurized cylinder. The two last options can operate in demand mode with varying levels of protection.

The results of this study showed that asbestos levels during outdoor removal tasks were lower than indoor work, but BZ concentrations were still up to 5 times higher than the current OEL. Ideally, work should be performed at or below 10 % of the OEL to ensure that workers are only exposed to acceptable levels below the OEL even at fluctuating concentrations. As a result, an APF of at least 50 is required for outdoor asbestos remediation work to ensure sufficient protection, based on findings in this study. As seen from Table 4, an APF of 50 is achieved for all full facepieces, some half masks, and some helmets and hoods, according to OSHA, thus providing an acceptable level of protection. In contrast, only SCBA solutions would give sufficient protection according to HSE. However, other studies in France and Norway have reported average BZ levels that were 67 times higher than the OEL during outdoor ACM removal (Ervik et al., 2023; Eypert-Blaison et al., 2018), in which case an APF of at least 670 is required. This limits options to some PAPR models as well as SAR and SCBA solutions not operating in demand mode. For indoor work, asbestos concentrations of up to 0.35 f/cm^3 were found, which is 100 times higher than the current OEL. Consequently, an APF of at least 1000 is required to achieve the necessary level of protection. This again limits the relevant RPE solutions to some PAPR models as well as SAR and SCBA solutions not operating in demand mode according to OSHA, while HSE finds that only SCBA solutions provide sufficient protection. However, as the recent EU directive requests a further lowering of the OEL to 0.002 f/cm^3, an APF higher than 1000 would be necessary to ensure worker exposure at maximum 10 % of the OEL.

Considerations for improved filter sampling and analysis

One of the main challenges in asbestos air sampling is to determine the optimal sampling time. The challenge arises from a combination of the newly lowered OEL and the risk of overloading filters in dusty environments. This combination means that a significant fraction of the overall filter has to be analyzed in order to report concentrations with the needed accuracy. It is therefore desired to sample as long as possible, but without overloading the filter, which is highly challenging, as the number and size of particles and fibers are not known when sampling.

Table 4
Guidance APF provided by HSE and OSHA for air-purifying respirator (APR), powered air-purifying respirator (PAPR), supplied-air respirator (SAR), and self-contained breathing apparatus (SCBA).

Type of mask	Mode of operation	Half mask		Full facepiece		Helmet/Hood		Loose-fitting facepiece	
		HSE	OSHA	HSE	OSHA	HSE	OSHA	HSE	OSHA
APR (P3)		20	10	40	50	–	–	–	–
PAPR		–	50	40	1000	40	25/1000	–	25
SAR	Demand	10	10	40	50	40		–	–
	Continuous flow	20	50	40	1000	40	25/1000	40	25
	Pressure-demand	–	50	–	1000	–		–	–
SCBA	Demand	–	10	2000	50	–	50	–	–
	Pressure-demand	–		2000	10.000	–	10.000	–	–

To visualize the challenge, Fig. 6 shows the number of images that must be analyzed in order to find 1 or 10 fibers, as a function of sampling time for two different scenarios. The two scenarios both used a sampling flowrate of 1.9 l/min and 8192 × 5632 pixel images. The first scenario (blue lines) corresponds to sampling at an asbestos concentration of 0.002 f/cm^3, which is one of the limits proposed in the recent EU Directive when only including fiber widths between 0.2 and 3 μm. Here a pixel resolution of 50 nm/pixel was set to reliably resolve 200 nm particles and fibers. The other scenario (red lines) assumes an asbestos concentration of 0.01 f/cm^3, which is the second option proposed in the EU directive. However, as this option includes fibers thinner than 200 nm, a pixel resolution of 12.5 nm/pixel was used, enabling reliable identification of particles and fibers down to 50 nm.

The necessary number of frames rises exponentially at short sampling times. This is a major challenge, since the high dust levels at construction sites typically limits sampling time to 0.5–2 h. As a result, hundreds of images must be analyzed from each sample, leading to a time consuming and expensive analysis. This highlights the need for automated approaches using artificial intelligence (AI) for fiber recognition. Automation with AI is a rapidly advancing field that could enable data collection and analysis overnight. However, it will require further development before fully or semi-automated AI work processes are fully operational.

Excluding fibers thinner than 200 nm allows a larger field of view per frame, resulting in a smaller analytical effort even with a lower OEL (Fig. 6). The 0.01 f/cm^3 option requires analysis of 3.2 times as many images as the 0.002 f/cm^3 option, making it far less favorable when measuring amphibole asbestos fibers, where TAF makes up only a small fraction of the overall distribution, according to this study. However, for chrysotile, where thin fibers may be more common (Ervik et al., 2023; Eypert-Blaison et al., 2018), the same conclusion cannot be definitively confirmed based on this study. In addition, as the 0.01 f/cm^3 option does not specify a lower fiber width limit, the magnification should in principle be increased further to include fibers thinner than 50 nm, which would require an even higher analytical effort. At the same time, the inclusion of thinner fibers will place a high demand on the equipment since not all SEMs can resolve objects at a few nm/pixel. Thus, the analysis will require a high-quality analytical SEM, again resulting in higher analytical costs. It is important but beyond this study to clarify what it means in relation to exposure measurements and preventive measures to include asbestos fibers thinner than 200 nm and to accept a higher OEL of 0.01 f/cm^3 rather than choosing the lower limit value and only including fibers with widths between 0.2 and 3 μm. Furthermore, it is necessary to determine whether the difference in fiber sizes influence the toxicological risk assessment and thus the health-based limit value. This includes both their hazard potential, but also the relative abundance of thinner fibers in the overall asbestos population.

Conclusion

Airborne asbestos concentrations were assessed from BZ, NF, and FF samples at 14 different construction and demolition sites, involving indoor and outdoor removal of ACM.

- Asbestos fibers were found in most of the collected dust samples and five asbestos types were identified with chrysotile being the most abundant.
  - In total 691 of 926 detected asbestos fibers fulfilled the WHO fiber criteria.
  - The overall asbestos fiber length distribution peaked at 5 μm, coinciding with WHO fiber length criteria. This makes asbestos fiber quantification sensitive to small shifts in asbestos length measurements. Reconsidering the length criteria for counting is recommended.
- Asbestos concentrations exceeded the current OEL in most tasks, even when considering 8-h TWA concentrations for the short sampling times (0.5–2 h). Highlights include:
  - Asbestos concentrations were lowest for outdoor tasks, but concentrations in BZ filters still exceeded the current Danish OEL.
  - The highest asbestos concentration was measured in the BZ during removal of tiles with asbestos adhesives and removal of ceiling panels.
  - The “bag method” used to wrap pipes with asbestos insulation before cutting, was found to reduce but not eliminate asbestos exposure.
  - Asbestos exposure levels during cleaning processes can exceed levels observed during ACM removal
- Considering observed asbestos concentrations, efficient RPE is needed in all work with asbestos

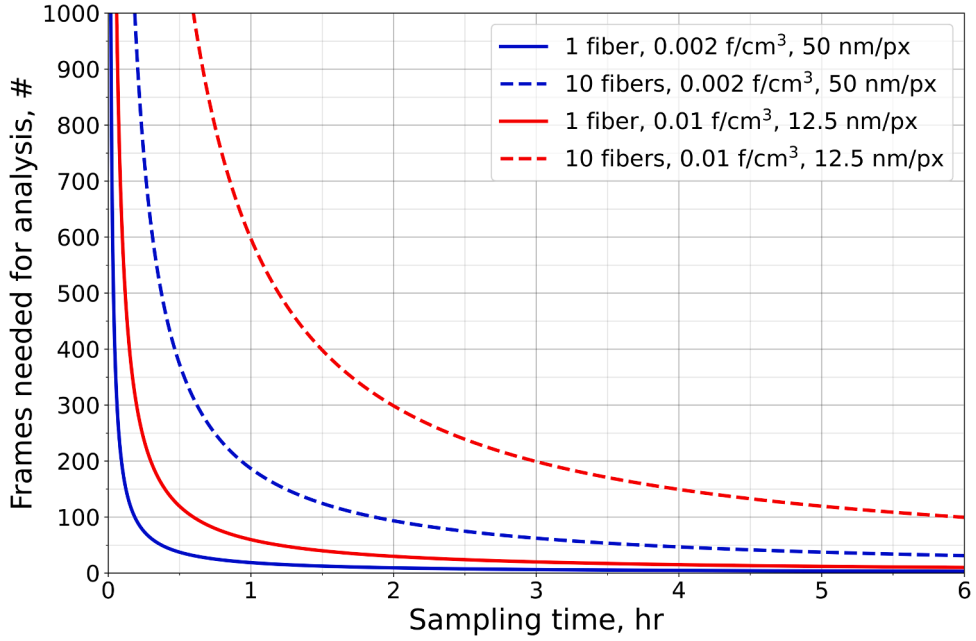

Fig. 6. Number of frames needed to find 1 or 10 fibers as a function of sampling time for two different scenarios based on options in the recent EU directive.

- RPE with a protection factor of at least 1000 was found necessary for indoor asbestos remediation and cleaning tasks based on the measured concentrations.
- RPE with a protection factor of 50 was found sufficient for outdoor work based on levels in this study, though other studies have found significantly higher outdoor levels.

- Challenges related to the two OEL options proposed in the recent EU directive were identified:
  - The 0.002 f/cm^3 OEL necessitates analysis of large filter areas in cases with low fiber count, especially when sampling small air volumes, which is required in dusty environments.
  - The 0.01 f/cm^3 OEL will result in a greater analytical burden than the alternative, due to very small FOW at the resolution required to identify fibers much thinner than 200 nm.
  - The 0.01 f/cm^3 OEL also faces challenges when measuring long fiber lengths at the high magnification required to resolve thin diameters.
  - Irrespective of OEL choice, fully or semi-automated AI driven analysis will be essential in the future for efficient asbestos analysis, which requires revision of current standards.

Funding sources

Sample collection was funded by the Danish Working Environment Authority (Arbejdstilsynet, AT), while sample and data analyses were funded by the Danish Working Environment Research Fund (AMFF, grant #47-2019-03). In addition the work was supported by FFIKA, Focused Research Effort on Chemicals in the Working Environment, a grant from the Danish government.

CRediT authorship contribution statement

Anders Brostrøm: Writing – original draft, Visualization, Validation, Software, Methodology, Investigation, Formal analysis, Data curation. **Henrik Harboe:** Visualization, Resources, Project administration, Methodology, Investigation, Data curation, Conceptualization. **Ana Sofia Fonseca:** Writing – review & editing, Supervision, Project administration, Methodology, Funding acquisition, Conceptualization. **Marie Frederiksen:** Writing – review & editing, Visualization, Project administration, Data curation. **Pete Kines:** Writing – review & editing, Software, Project administration, Formal analysis, Data curation. **William Bührmann:** Writing – review & editing, Methodology, Formal analysis. **Jakob Hjort Bønløkke:** Writing – review & editing, Visualization, Resources, Project administration, Funding acquisition, Conceptualization. **Keld Alstrup Jensen:** Writing – review & editing, Visualization, Supervision, Resources, Project administration, Funding acquisition, Conceptualization.

Declaration of competing interest

The authors declare that they have no known competing financial interests or personal relationships that could have appeared to influence the work reported in this paper.

Supplementary materials

Supplementary material associated with this article can be found, in the online version, at doi:10.1016/j.hazadv.2024.100552.

Data availability

The result data and relevant information for each of the analyzed filter samples is available in the Excel file submitted as supplementary material. This data is the basis for the presented work.

References

Andersen, L.P., Nørdam, L., Joensson, T., Kines, P., Nielsen, K.J., 2018. Social identity, safety climate and self-reported accidents among construction workers. Constr. Manag. Econ. 36, 22–31. https://doi.org/10.1080/01446193.2017.1339360.

Barlow, C.A., Grespin, M., Best, E.A., 2017. Asbestos fiber length and its relation to disease risk. Inhal. Toxicol. 29, 541–554. https://doi.org/10.1080/08958378.2018.1435756.

Ervik, T., Eriksen Hammer, S., Graff, P., 2021. Mobilization of asbestos fibers by weathering of a corrugated asbestos cement roof. J. Occup. Environ. Hyg. 18, 110–117. https://doi.org/10.1080/15459624.2020.1867730.

Ervik, T.K., Hammer, S.E., Skaugset, N.P., Graff, P., 2023. Measurements of airborne asbestos fibres during refurbishing. Ann. Work Expo. Health 67, 952–964. https://doi.org/10.1093/annweh/wxad041.

Eypert-Blaison, C., Romero-Hariot, A., Clerc, F., Vincent, R., 2018. Assessment of occupational exposure to asbestos fibers: contribution of analytical transmission electron microscopy analysis and comparison with phase-contrast microscopy. J. Occup. Environ. Hyg. 15, 263–274. https://doi.org/10.1080/15459624.2017.1412583.

Fonseca, A.S., Jørgensen, A.K., Larsen, B.X., Moser-Johansen, M., Flachs, E.M., Ebbehøj, N.E., Bønløkke, J.H., Østergaard, T.O., Bælum, J., Sherson, D.L., Schlünssen, V., Meyer, H.W., Jensen, K.A., 2022. Historical asbestos measurements in Denmark—A national database. Int. J. Environ. Res. Public Health 19, 643. https://doi.org/10.3390/ijerph19020643.

Harris, E.J.A., Lim, K.P., Moodley, Y., Adler, B., Sodhi-Berry, N., Reid, A., Murray, C.P., Franklin, P.J., Musk, A.(Bill), de Klerk, N.H., Brims, F.J.H., 2021. Low dose CT detected interstitial lung abnormalities in a population with low asbestos exposure. Am. J. Ind. Med. 64, 567–575. https://doi.org/10.1002/ajim.23251.

Hendry, N.W., 1965. The geology, occurrences, and major uses of abestos. Ann. N. Y. Acad. Sci 132, 12–21. https://doi.org/10.1111/j.1749-6632.1965.tb41086.x.

HSE, 2013. Respiratory Protective Equipment at Work: A Practical Guide, fourth ed. HSE Books, London.

Ilgren, E.B., Hoskins, J.A., 2017. Anthophyllite asbestos: the role of fiber width in mesothelioma induction part 1: epidemiological studies of Finnish anthophyllite asbestos. Environ. Pollut. 7, 9. https://doi.org/10.5539/ep.v7n1p9.

INRS (Institut National de Recherche et de Sécurité), 2011. Les appareils de protection respiratoire, choix et utilisation [WWW Document]. URL https://www.esst-inrs.fr/3rb/ressources/ed6106.pdf.

Iversen, I.B., Vestergaard, J.M., Ohlander, J., Peters, S., Bendstrup, E., Bonde, J.P.E., Schlünssen, V., Bønløkke, J.H., Rasmussen, F., Stokholm, Z.A., Andersen, M.B., Kromhout, H., Kolstad, H.A., 2024. The asbestos–asbestosis exposure–response relationship: a cohort study of the general working population. Scand. J. Work Environ. Health 50, 372–379. https://doi.org/10.5271/sjweh.4153.

Janssen, L., Zhuang, Z., Shaffer, R., 2014. Criteria for the collection of useful respirator performance data in the workplace. J. Occup. Environ. Hyg. 11, 218–226. https://doi.org/10.1080/15459624.2013.852282.

Miljøstyrelsen, 2023. Udvikling af teknologi til sikker identifikation af asbestfri eternitplader.

Occupational Safety and Health Administration (OSHA), 2009. Assigned Protection Factors for the Revised Respiratory Protection Standard [WWW Document]. www.osha.gov. URL https://www.osha.gov/sites/default/files/publications/3352-APF-respirators.pdf (accessed 8.26.24).

Paris, C., Thierry, S., Brochard, P., Letourneux, M., Schorle, E., Stoufflet, A., Ameille, J., Conso, F., Pairon, J.C., the National APEXS Members, 2009. Pleural plaques and asbestosis: dose- and time-response relationships based on HRCT data. Eur. Respir. J 34, 72–79. https://doi.org/10.1183/09031936.00094008.

Pawełczyk, A., Božek, F., 2015. Health risk associated with airborne asbestos. Environ. Monit. Assess. 187, 428. https://doi.org/10.1007/s10661-015-4614-3.

Peters, T., Schumann, J., Stange, M., Bäger, D., Broßell, D., Dziurowitz, N., Kämpf, K., Thim, C., Meyer-Plath, A., 2024. AI-assisted identification, morphological characterisation and quantification of micro- and nanoscale asbestos, microplastic and carbon fibres for human and environmental exposure control. In: Arbeitsgruppe Ressortforschung: Symposium Und Mitgliederversammlung. Presented at the Arbeitsgruppe Ressortforschung: Symposium und Mitgliederversammlung. Berlin.

Raffn, E., Lynge, E., Juel, K., Korsgaard, B., 1989. Incidence of cancer and mortality among employees in the asbestos cement industry in Denmark. Occup. Environ. Med. 46, 90–96. https://doi.org/10.1136/oem.46.2.90.

Ramada Rodilla, J.M., Calvo Cerrada, B., Serra Pujadas, C., Delclos, G.L., Benavides, F.G., 2022. Fiber burden and asbestos-related diseases: an umbrella review. Gac. Sanit. 36, 173–183. https://doi.org/10.1016/j.gaceta.2021.04.001.

Rasmussen, T.V., 2010. SBI-anvisning 229: "Byggematerialer med asbest" [WWW Document]. www.at.dk. URL https://at.dk/arbejdsmiljoe/asbest/asbest-i-arbejdsmiljoeet/byggematerialer-med-asbest/ (accessed 8.26.24).

Rueden, C.T., Schindelin, J., Hiner, M.C., DeZonia, B.E., Walter, A.E., Arena, E.T., Eliceiri, K.W., 2017. ImageJ2: ImageJ for the next generation of scientific image data. BMC Bioinform. 18 (529). https://doi.org/10.1186/s12859-017-1934-z.

Strohmeier, B.R., Huntington, J.C., Bunker, K.L., Sanchez, M.S., Allison, K., Lee, R.J., 2010. What is asbestos and why is it important? Challenges of defining and characterizing asbestos. Int. Geol. Rev. 52, 801–872. https://doi.org/10.1080/00206811003679836.

Suzuki, Y., Yuen, S.R., Ashley, R., 2005. Short, thin asbestos fibers contribute to the development of human malignant mesothelioma: pathological evidence. Int. J. Hyg. Environ. Health 208, 201–210. https://doi.org/10.1016/j.ijheh.2005.01.015.

The European Parliament and the Council of the European Union, 2023. Directive (EU) 2023/2668 of the European parliament and of the council of 22 November 2023

amending directive 2009/148/EC on the protection of workers from the risks related to exposure to asbestos at work. Official J. Eur. Union.

Thives, L.P., Ghisi, E., Thives Júnior, J.J., Vieira, A.S., 2022. Is asbestos still a problem in the world? A current review. J. Environ. Manag. 319, 115716. https://doi.org/10.1016/j.jenvman.2022.115716.

Van Gosen, B.S., 2007. The geology of asbestos in the United States and its practical applications. Environ. Eng. Geosci. 13, 55–68. https://doi.org/10.2113/gseegeosci.13.1.55.